Available online at www.sciencedirect.com
SCIENCE DIRECT
ELSEVIER
Journal of the European Ceramic Society 25 (2005) 1943–1952
EC§RS
www.elsevier.com/locate/jeurceramsoc

The behavior of the oxide-coated Nicalon^{TM} fibers exposed to air at 1000 °C

T.M. Zima[a], N.I. Baklanova[a,*], A.T. Titov[b]

[a] Institute of Solid State Chemistry and Mechanochemistry SB RAS, Kutateladze st. 18, Novosibirsk 630128, Russian Federation
[b] General Institute of Geology, Geophysics and Mineralogy SB RAS, Novosibirsk 630090, Russian Federation

Received 25 February 2004; received in revised form 6 June 2004; accepted 20 June 2004

Abstract

The behavior of Nicalon^{TM} fibers with sol–gel derived alumina, zirconia and alumina/zirconia interfacial coatings exposed to air at 1000 °C was studied. Kinetic measurements of the oxidation rates of Nicalon^{TM} fibers with coatings derived from different routes were conducted. Morphology, texture and composition of oxide-coated Nicalon^{TM} fibers after exposition were studied using SEM, EDS, XRD, and XPS analysis. Some common and distinctive features of the behavior were found. In all cases the oxidation is satisfactorily described by the oxygen diffusion-controlled mechanism. Some peculiarities of behavior of oxide interfacial coatings in dependence on type oxides and their prehistory are discussed. The oxide-based interfacial coatings can be considered as promising ones but their properties must be optimized to increase the oxidation resistance of Nicalon^{TM} fibers.

Keywords: Interfaces; Nicalon fiber; Sol–gel processes; Oxidation

1. Introduction

Fiber-reinforced ceramic composites achieve high toughness through the distributed damage mechanisms. These mechanisms are dependent on matrix cracks deflecting into fiber/matrix interfacial debonding cracks.[1] Crack deflection in most CMC's reinforced by SiC-based fibers such as Nicalon^{TM}, Hi-Nicalon^{TM}, Sylramic® is achieved through the disposal of weak and compliant carbon or BN interfacial coatings.[2–5] However, these interfaces have proved to be susceptible to oxidation at intermediate temperatures and rapidly lose their effectiveness. The fundamental limitations of carbon and BN make them the life-limiting constituent for most composite systems. Therefore, the oxidation problem of interfacial coatings is considered to be one the most important problems remaining to be solved before SiC/SiC composites can be reliably introduced in the next generation aircraft engines, space vehicles, gas turbines, and other applications.[6]

The instability of the common interface materials such as carbon and boron nitride has motivated research on more oxidation-resistant fiber coatings.[7–12] It is commonly believed that oxide coatings represent the best choice in terms of oxidation resistance.[6] Although it is true for the prevention of oxidation coatings, it is no necessary to be true for the protection of the underlying non-oxide fibers and matrixes (SiC-based) from oxidation or for weak fiber/matrix bonding. It should be suggested that a complex interphase materials criteria may not be easily satisfied by refractory compounds. However, there are several positive examples of refractory oxides as suitable interphase materials for non-oxide composites.[9,11–16]

In previous work[17] we studied the particularities of the formation of the ZrO_2, TiO_2, Al_2O_3 and double oxide interfacial coatings on Nicalon^{TM} fiber by sol–gel technique. Our approach to fabrication of these coatings was based on usage of aqueous sols of corresponding oxides. Water is one of components not only of aqueous sols but organometallic sols and solutions, which are usually used to coat ceramic fibers and composite materials with refractory oxides.[14–17] In some

---

* Corresponding author. Tel.: +7 3832 363839; fax: +7 3832 322847.
E-mail address: baklanova@solid.nsc.ru (N.I. Baklanova).

0955-2219/$ – see front matter © 2004 Elsevier Ltd. All rights reserved.
doi:10.1016/j.jeurceramsoc.2004.06.011

cases, pre-treatment of Nicalon^{TM} fabrics before testing or characterization includes the immersion of fibers into warm water to remove a sizing.[18] Further, an "accelerated" oxidation of SiC-based materials in high temperature, high steam environment was well-documented (see, e.g.[19–21]). One can propose, that water is an important factor to be taken into consideration. The objective of present study was (i) to examine the oxidation of refractory oxide-coated fibers exposed to air at 1000 °C and (ii) to evaluate the influence of some factors, among them, disperse medium (water) on the mechanism of oxidation. Of course, oxidation resistance should be considered in terms of the overall composite system to determine how oxidation degrades composite properties and how system, including the fiber, coating and matrix can be modified to alleviate this problem. Nevertheless, a study of oxidation resistance of coated Nicalon^{TM} fibers exposed to air at high temperatures for a long time is of great interest. This situation can be realized under extreme conditions when the open ends of coated fibers are exposed to the surrounding atmosphere or when matrix cracks are present, allowing atmospheric oxygen to reach the fiber coatings.

2. Experimental

2.1. Substrate preparation

Woven Nicalon^{TM} NLM202 (Nippon Carbon Co. Japan) fiber cloths were used as substrate materials. Prior to coating, Nicalon^{TM} fiber cloths were immersed for 24 h in 50:50 acetone/ethanol mixture for removing a sizing agent, after that they were dried at ambient temperature. Then they were thermally treated in air at 450 °C.

2.2. Coating preparation

Precursors for single and multicomponent refractory oxide coatings were the sols of hydrated aluminium and zirconium dioxide. The sols were synthesized by electrochemically at 60–65 °C from 1 M aqueous solutions of metal oxychlorides using diaphragmless electrolyzer with platinum Fisher's electrodes. The time was about 2 h. The chloride ion content was monitored in course of synthesis by standard procedure. The concentration of disperse phase was varied by diluting with water before coating procedure. The coating stage involved firstly the immersion of the fiber fabrics into sols. When fiber tows or woven fibers are used, the coating procedure becomes more difficult because of single monofilaments in close proximity are difficult to coat uniformly and the problem of bridging of fibers by coating arises. So special procedure developed by us was applied to facilitate the sol infiltration into the woven architecture. This procedure was similar to that one described by Gu et al.[22] Then, the fiber clothes were exposed to air at ambient temperature. Thermal treatment was optimized in order to obtain crack free coatings. The specimens were slowly (5 °C/min) heated till 960 °C in vacuum ~1 Pa. To increase of thickness of interfacial coating the dipping–annealing procedure was repeated. Herein after, the coatings derived from diluted sols are denoted as "d" and from undiluted as "ud". The number of dipping–annealing cycles is denoted with arabic numerals.

Two approaches were applied to fabrication of complex oxide coatings. In accordance with one of them, the sols were synthesized separately and then mixed in 1:1 volume ratio before deposition process (type I). The second approach comprised the electrochemical synthesis of sol from aqueous solution of two different metal oxychlorides (type II).

A special procedure was applied to some specimens of Nicalon^{TM} cloths before oxidation tests. After desizing in accordance with procedure mentioned in Section 2.1, the specimens were dipped into distilled water, maintained for several minutes, drawn out and dried at ambient temperature until no changing of mass. Then they were heated in vacuum at 960 °C for 1 h, cooled and weighted. The total mass loss after this procedure was below 3 wt.%.

2.3. Oxidation tests

The oxidation behavior of coated and uncoated Nicalon^{TM} fabrics was examined in air under static conditions. All of experiments were carried out at 1000 °C. The samples of Nicalon^{TM} fabrics (100–200 mg) were placed in the furnace (KO-14, German) heated preliminary to 1000 °C and kept during a definite time interval. Then the samples were taken out, cooled in dessicator and weighted with accuracy ±0.1 mg. A total time of testing was 30 h.

2.4. Specimen characterization

The phases in coatings were characterized by X-ray diffraction analysis (XRD) using monochromatic Cu Kα radiation with DRON-3 diffractometer (Russia). Scanning electron microscopes (JSM T-20, Jeol, BF-350, Tesla, and SEM LEO 1430VP, supplied by EDX Oxford spectrometer) were used for coating morphology characterization.

The electronic structure of coating before and after oxidation was characterized by XPS using VG ESCALAB spectrometer. XPS spectra were recorded using Al Kα irradiation. All spectra are presented in binding energy scale obtained with respect to C 1s peak of carbon at 284.8 eV.

The specific surface area of desized Nicalon fibers before and after water treatment was determined by BET method. Before measurements the samples were heated at 120 °C in Ar/He flow.

3. Results

3.1. Oxidation tests

Dependence of the relative mass $(\Delta m)^2/m$ on time at 1000 °C for uncoated Nicalon^{TM} fibers preliminary treated

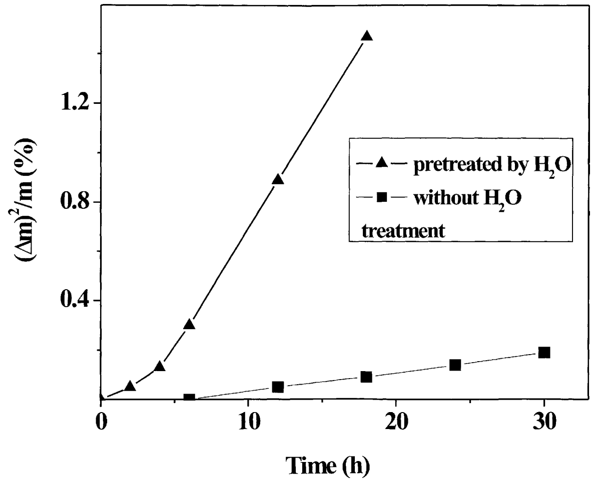

Fig. 1. Dependence of the relative mass $(\Delta m)^2/m$ on time at 1000 °C for uncoated Nicalon^{TM} fibers preliminary treated under different conditions.

under different conditions is represented in Fig. 1. One can see, that for desized Nicalon^{TM} fibers an insignificant mass gain is observed only after the 6 h exposition to air. Preliminary treatment by water of desized Nicalon^{TM} fibers results in a significant increase of the oxidation rate of samples. The $(\Delta m)2/m$–time dependence obeys the linear law that confirms the parabolic oxidation law characteristic of a diffusion-controlled mechanism.

The $(\Delta m)^2/m$–time plots for Al_2O_3-coated Nicalon^{TM} fibers exposed to air at 1000 °C are shown in Fig. 2. One can see, that linear dependence for Al_2O_3 (d, 1)-coated Nicalon^{TM} is observed. The oxidation rates of Nicalon^{TM} fibers with Al_2O_3 coating derived from diluted and undiluted sols are greatly distinguished from each other, namely, for whole period of exposition the oxidation rate for Al_2O_3 (d)-coated Nicalon^{TM} is higher than for Al_2O_3 (ud)-coated fibers.

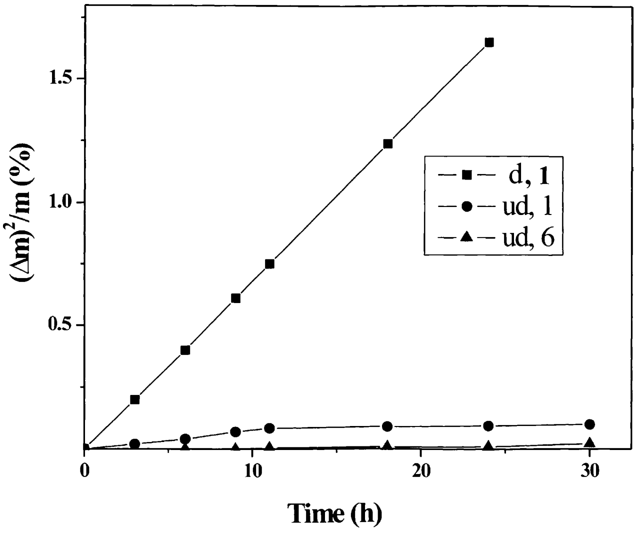

Fig. 2. Dependence of the relative mass $(\Delta m)^2/m$ on time at 1000 °C for Nicalon^{TM} fibers with Al_2O_3 coating.

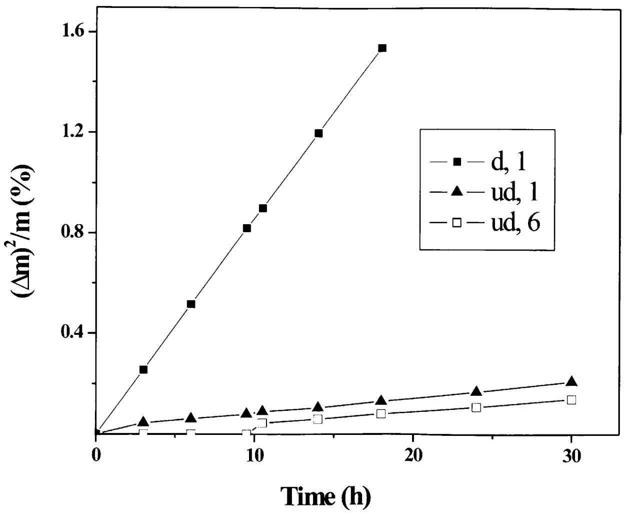

Fig. 3. Dependence of the relative mass $(\Delta m)^2/m$ on time at 1000 °C for Nicalon^{TM} fibers with ZrO_2 coating.

The $(\Delta m)^2/m$–time plot for oxidation of the Al_2O_3 (ud, 1)-coated Nicalon^{TM} fiber reveals two regions with different slopes (before and after the 11 h exposition). An increase of the number of dipping–annealing cycles up to six leads to a sharp decrease in the oxidation rate.

A similar picture is observed for ZrO_2-coated Nicalon^{TM} fibers during exposition to air (Fig. 3). One can see, that dependence of $(\Delta m)^2/m$ on time for ZrO_2 (d)-coated Nicalon^{TM} fibers obeys the linear law. The dilution of the ZrO_2 sols which are used for coating process results in an increasing of oxidation rate of coated fibers. The peculiarity of behavior of ZrO_2 (three to six cycles)-coated Nicalon^{TM} fibers is an appearance of a noticeable mass gain only after 10 h from the beginning of exposition (Fig. 3).

The results of oxidation of the Al_2O_3–ZrO_2-coated Nicalon^{TM} fibers as plots of $(\Delta m)^2/m$–time are represented in Fig. 4. One can see, that the Al_2O_3–ZrO_2 (type II)-coated

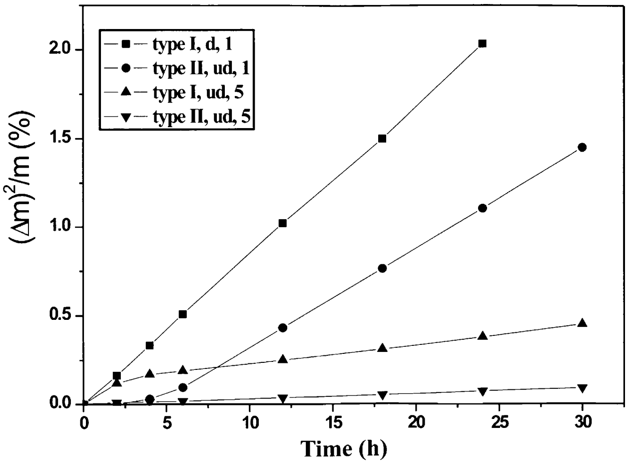

Fig. 4. Dependence of the relative mass $(\Delta m)^2/m$ on time at 1000 °C for Nicalon^{TM} fibers with the Al_2O_3–ZrO_2 coating.

Nicalon^{TM} fibers are oxidized slowly than type I. An increase of number of dipping–annealing cycles in course of the fabrication of the Al_2O_3–ZrO_2 (both type I and type II soles)-coated Nicalon^{TM} fibers results in an increase of oxidation resistance of coated fibers.

Summing up the data on kinetics of oxidation of oxide-coated Nicalon^{TM} fibers, one can emphasize the following peculiarities of their behavior under exposition to air at 1000 °C. Firstly, oxidation rates are depend on concentration of sols which are used for the fabrication of coatings. Usage of concentrated sols results in retarding of oxidation of coated fibers. Secondly, the oxidation resistances of coated (with diluted sols) fibers only slightly differ from each other. Thirdly, the oxidation resistance of Nicalon^{TM} fibers with Al_2O_3/ZrO_2-based coatings depends on sol–gel routes that are used for their formation.

3.2. SEM analysis

SEM images of the surface and the cross-section of Nicalon^{TM} fibers preliminary treated by water and then exposed to air at 1000 °C are represented in Fig. 5a–c. Nicalon fibers exposed to air without prior water treatment show new surface features as separate well-developed crystals. However, the fibers annealed in air after water treatment showed scale formation on the surface. The scale is rather uniform, smooth and highly porous one. The size of particles and pores, determined from the SEM micrographs with the Image-Pro Plus software, is about 20–60 nm. Separate well-developed crystals can be observed at the edge of cross-section of some fibers.

SEM images of the surface and the cross-section of Al_2O_3 (d, 1)-coated Nicalon^{TM} fibers before and after exposition to air at 1000 °C are represented in Fig. 6a–c. The surface of oxidized filaments resembles jigsaw puzzle. The columnar microstructure of coating after oxidation is apparent. Growing crystals are parallel and directed normally to the fiber surface, i.e. the coating is textured. One can see, that some of columns are joined each other in outer part of coating. The thickness determined from SEM images is about 1 μm. No visible coating-fiber interfacial zone was detectable with SEM analysis. One can see that open long pores with sizes of several nanometers across and about 1 μm long are appeared between columnar crystals. Beside pores, other macro defects including the new formations of rounded shape with 0.5–1 μm in diameter and cavities can be observable.

SEM images of the surface of Al_2O_3 (ud, 1)-coated Nicalon^{TM} fibers before and after exposition to air at 1000 °C are represented in Fig. 7a–c. Unlike the coating derived from diluted Al_2O_3 sol, this coating is dense, glass-like one with numerous macro defects, such as cracks, large sized well-developed crystals, dendrites and other nonuniformaties. According to EDX measurements, the composition of crystals is represented by Al, Si, and O. Longitudinal long cracks and spalling of coating are observed.

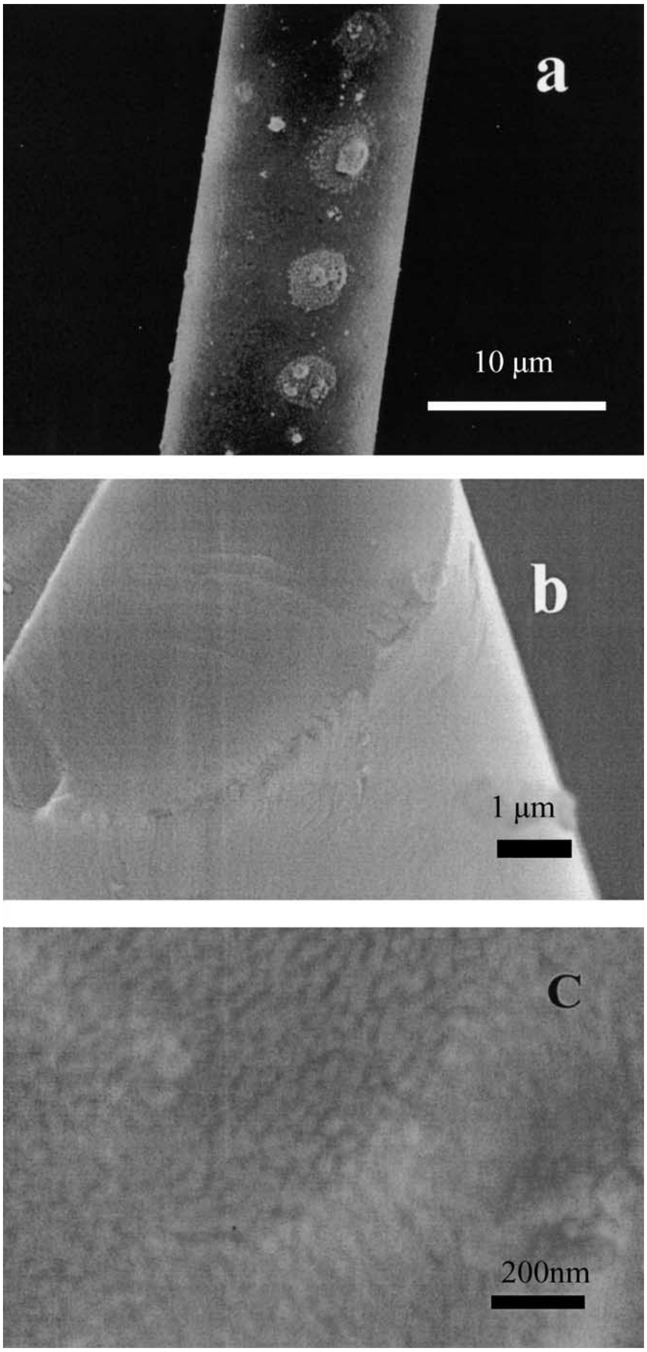

Fig. 5. (a–c) SEM images of the surface of desized and exposed to air at 1000 °C (a); treated by water and exposed to air at 1000 °C (b and c).

SEM micrographs of the ZrO_2 (d)-coated Nicalon^{TM} fibers after exposition to air at 1000 °C are represented in Fig. 8a and b. The coating is a very smooth, uniform and adherent. An exposure of ZrO_2-coated fibers to air results in healing of defects and smoothing of surface. The coating is built from columns that are directed normally to the surface of filament. However, a column structure is denser in comparison with one for the alumina coating (Fig. 6c). The thickness of coating after oxidation is about 1 μm. No coating spallation was observed for whole period oxidation.

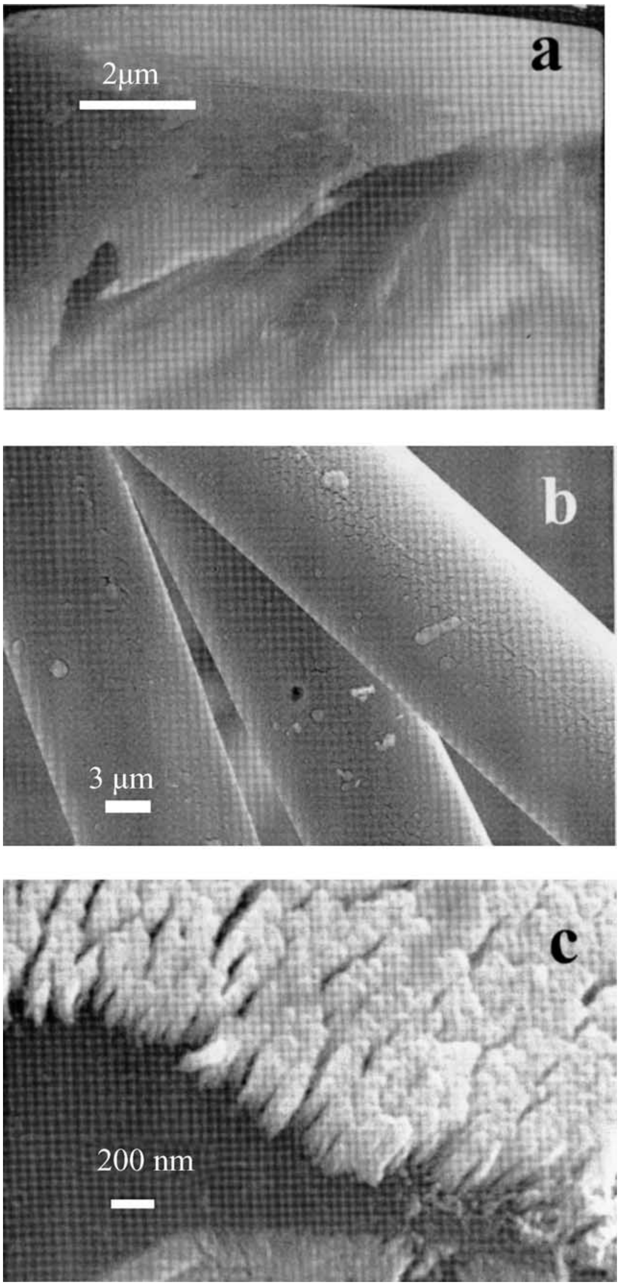

Fig. 6. (a–c) SEM images of the surface and the cross-section of Al_2O_3 (d, 1)-coated Nicalon^{TM} fibers before (a) and after exposition to air at 1000 °C (b and c).

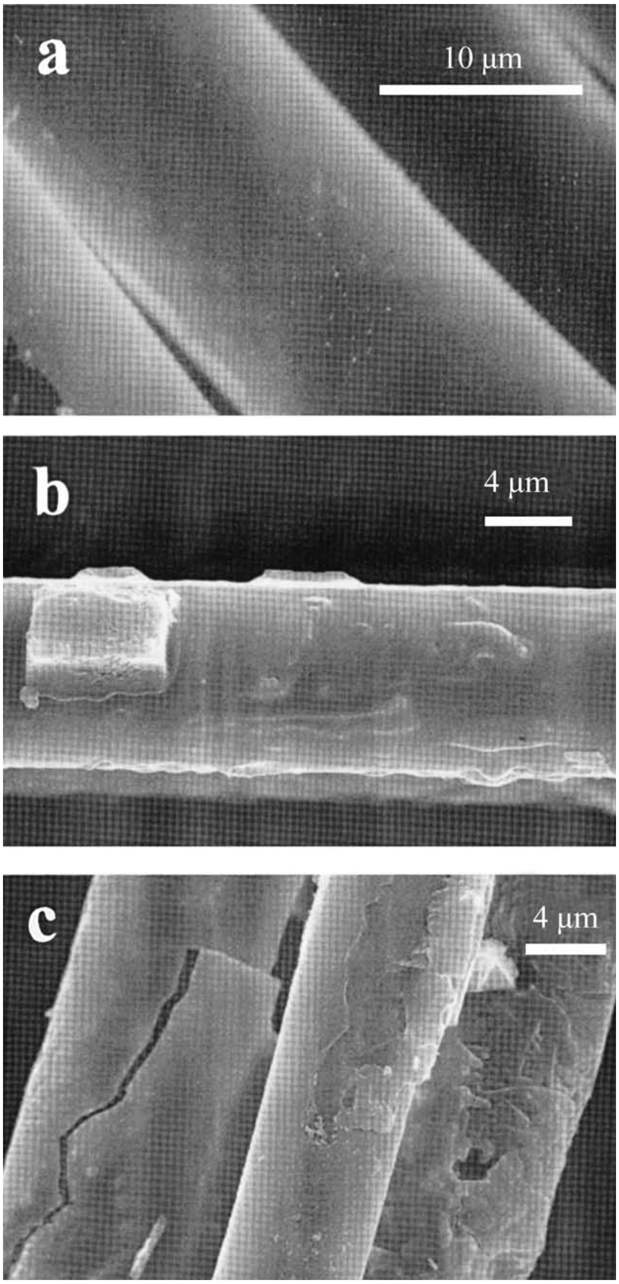

Fig. 7. (a–c) SEM images of Al_2O_3 (ud, 1)-coated Nicalon^{TM} fibers before (a) and after exposition to air at 1000 °C (b and c).

3.3. XPS and XRD analysis

XPS survey spectra recorded from oxidized coated and uncoated Nicalon^{TM} fabrics revealed carbon, silicon, oxygen, zirconium, aluminum as main components. The common feature of oxidized coated Nicalon^{TM} fibers is the presence of silicon dioxide as main component. Asymmetry and slight shift of the O 1s photopeak for oxidized oxide-coated fibers in comparison with oxidized uncoated fibers are an evidence of heterogeneity of oxidized coatings and the presence of oxide phases other than SiO_2 (Fig. 9a and b). In the XPS spectrum (Fig. 9a, curve 4) a distinctive shoulder is present. The location of this peak is in accordance with the value for ZrO_2 reported by Moulder et al.[23] The XPS spectra confirm the presence of aluminum and zirconium in the Al_2O_3-, ZrO_2- and Al_2O_3/ZrO_2 coatings derived from diluted sols by one-fold dipping (Fig. 10a and b).

The results of XRD studies of coated Nicalon^{TM} fibers exposed to air are shown in Fig. 11. It should be noted that an assignment of peaks in the XRD patterns of oxide-coated Nicalon^{TM} fibers is a rather difficult. This is due to several reasons. Firstly, these coatings are very thin, nanosized and poorly crystallized and as result, weak intensities are ob-

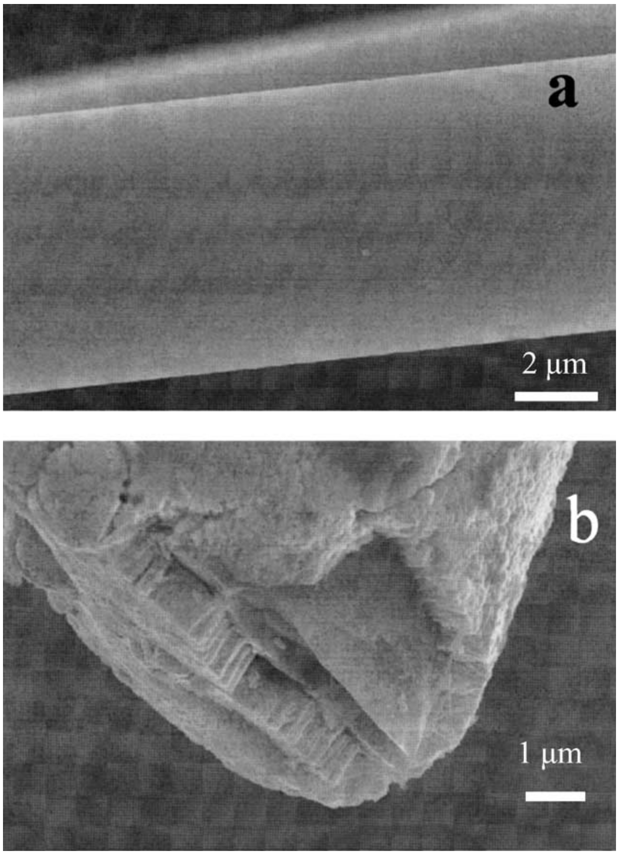

Fig. 8. (a and b) SEM images of the ZrO_2 (d, 1)-coated Nicalon^{TM} fibers after exposition to air at 1000 °C.

served in the XRD patterns. Secondly, the positions of XRD peaks of phases comprising the coatings are very closely to each other and besides, they are superposed to the β-SiC phase peaks of Nicalon^{TM} fiber itself. This is why the interpretation of obtained experimental data is an ambiguous one.

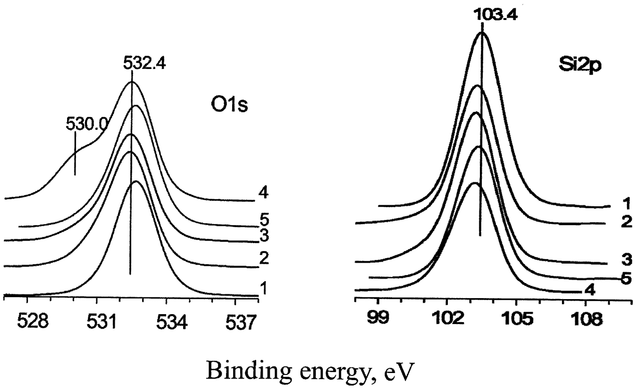

Fig. 9. XPS spectra for oxidized Nicalon^{TM} fiber: O 1s and Si 2p photopeaks for uncoated (1) and coated Nicalon (2–5): Al_2O_3 (2); Al_2O_3, d (3); ZrO_2 (4); Al_2O_3/ZrO_2 (5).

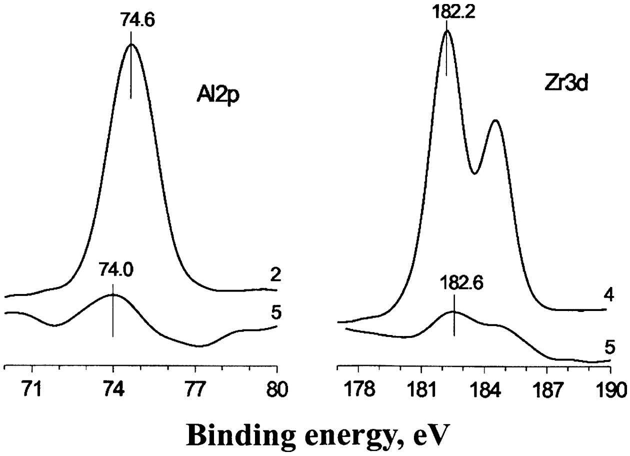

Fig. 10. Al 2p and Zr 3d photopeaks of the oxidized Al_2O_3-, ZrO_2-, and Al_2O_3/ZrO_2-coated Nicalon^{TM} fibers.

The Al_2O_3 (ud, 6) coating remains X-ray amorphous after long exposition to air and only wide diffuse peaks of β-SiC can be observed. In the XRD patterns of ZrO_2-coated Nicalon^{TM} fiber before and after exposition in air peaks belonging to tetragonal and monoclinic modifications of ZrO_2 are present,[24] the m-ZrO_2 being a predominant. As was mentioned early by Baklanova et al.,[17] in the XRD patterns of the Al_2O_3–ZrO_2 (type I, ud, 5)-coated Nicalon^{TM} fibers only peaks belonging to t-ZrO_2 were detected. After exposition of the Al_2O_3–ZrO_2-coated Nicalon^{TM} fibers to air besides the peaks of t-ZrO_2, the other features that could be assigned to $ZrSiO_4$ were also observed.

The weak peaks for the Al_2O_3–ZrO_2 (type II, 5 cycles)-coated fibers were observed in the XRD patterns. They appear to belong to t- or c-ZrO_2 phase. After oxidation the appearance of additional weak feature that could be ascribed to the Al_2O_3 phase became noticeable (Fig. 11).

4. Discussion

Several results concerning the behavior of oxide-coated Nicalon^{TM} fibers must be discussed in detail. The first group of results is connected with the stability of uncoated fibers exposed to water prior to oxidation tests. The above kinetic experiments clearly show that Nicalon^{TM} fibers are not stable when exposed to water and then annealed at 1000 °C in air. Clearly, that the exposure to water before oxidation tests is critical moment to the increase in the rate of oxidation. As an oxidation process is heterogeneous one it was proposed that the surface of Nicalon^{TM} fiber is affected by water treatment even at ambient temperature. The structure and composition of Nicalon^{TM} fiber and its surface were a question under investigation of numerous publications (see, e.g.[25–27]). It was shown that the fiber appears to be composed of a "continuum" of SiC_4 and SiC_xO_y tetrahedrons. In addition, graphite like carbon structures would be present. On the fiber surface there is a very thin SiO_2 (about 10 nm) layer, the bulk of fiber being not concerned with this layer.[25]

It could be proposed the different mechanisms of influence of preliminary water treatment on accelerated oxidation

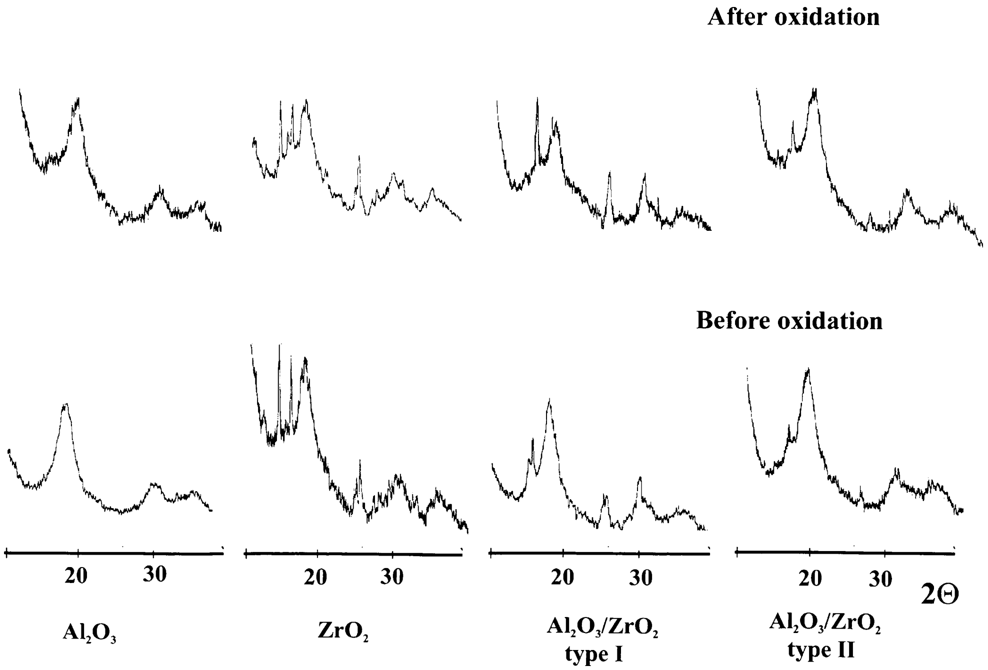

Fig. 11. XRD patterns of oxide-coated Nicalon™ fibers before and after exposition to air at 1000 °C.

of Nicalon™ fiber in air. One of them is based on the fact that on the SiO_2 surface the Si-OH groups are present. They provide a chemisorption of H_2O molecules on the SiO_2 surface. Heating of fiber pretreated with water results in the elimination of H_2O molecules and the formation of highly porous structure of the SiO_2 surface layer. The BET measurements showed the ~20–25% increase in specific surface area of desized and pretreated by water Nicalon™ fiber in comparison with untreated desized fiber. Further, it is well-documented,[28] that an amorphous SiO_2 has a noticeable solubility in water at neutral pH[28] and at ambient temperature. So it must not be excluded that dipping of fibers into distilled water could result in a partial solubility and distortion of integrity of the thin SiO_2 surface layer.

The different character of oxidation for both types of uncoated fibers is also clearly seen in their SEM images (Fig. 5a and b). "Islets" of finely crystalline phase are formed on the untreated surface of fiber in contradiction to uniform, highly porous coating of fiber pretreated by water. A distinguished morphology of both types (treated and untreated by water) fibers can be also a reason of difference in the oxidation kinetics. Actually, highly porous textured silica coating allows more rapid diffusion of gaseous substances along grain boundaries. As a result, we observe accelerated oxidation rates for fiber pretreated by water.

The other group of results to be discussed is an oxidation of Nicalon™ fibers with coatings derived from diluted sols. As one can see from Figs. 1–3, the oxidation rates of these coated Nicalon™ fibers are only slightly lowered in comparison with those of uncoated Nicalon™ fibers pretreated by water. It is no unexpected result and two reasons must be taken into consideration. Firstly, diluted sols contain a large quantity of disperse medium, namely, water. In other words, the process of the formation of coatings with one-fold dipping into diluted sols, in some extent, is an analog to the pre-treatment of fibers by water. Secondly, the initial (before oxidation) oxide coatings derived from diluted sols (one cycle) are very thin and porous ones, the pore and particle sizes being about 30–50 nm, as was early reported by Baklanova et al.[17] After oxidation the microstructures of coatings of oxidized Al_2O_3- and ZrO_2-coated Nicalon™ fibers are columnar ones, long open pores directed normally to the surface and micro cracks present. One can propose that these microstructures will provide a diffusion of oxygen inward to the fiber-coating interface along grain boundaries and cracks and this mechanism is predominant at as low temperature as 1000 °C. So effectiveness of them to protect underlying fiber from further oxidation is not so high and only slightly differs from each other.

According to Jarvis and Carter,[29] adhesion energy at the ZrO_2/SiO_2 interface is quite high. They calculated that a very strong bonding and a dramatic rearrangement of the atomic coordinates exist at this interface and concluded that chemical bonding provides a significant source of interface strengthening even at ambient temperature and in the absence of a new reaction phase. From this point of view, such coating might exhibit improved resistance to debonding and subsequent spallation under thermal cycling conditions. Actually, no spallation of the ZrO_2 coating derived from diluted sols exposed to air at 1000 °C was observed, as one can see from Fig. 8.

The third group of results is connected with the behavior of Nicalon™ fibers coated by oxides derived from undiluted sols and exposed to air at 1000 °C. As one can see from Figs. 1–4, a rather strong slowing of oxidation of coated fibers in comparison with uncoated (Fig. 1, curve 1) is observed. Further, a decrease in the oxidation rates is detected for fibers coated with undiluted sol in comparison with those coated with diluted for the same oxide(s) and the same number of cycles. A SEM observation of microstructures of these coatings suggests that the formation of dense, porousless, glass-like layers can be considered as main reason of slowing.

During exposition to air of oxide (ud)-coated fibers the inward diffusion of oxygen will proceed through several stages including oxygen diffusion through the dense oxide (ZrO_2, Al_2O_3 or ZrO_2/Al_2O_3) layer, then through the very thin surface SiO_2 layer to SiC, where the oxidation reaction occurs. As product of oxidation, namely, silica is formed, oxygen must diffuse through it to arrive unoxidized SiC. Because of the oxidation rate is controlled by the slowest stage, the diffusion through either the metal oxide or silica layer will be the rate-limiting stage in dependence of the oxygen diffusivity values.

It could be proposed that for Al_2O_3 (ud)-coated Nicalon^{TM} fibers the diffusion through the Al_2O_3 layer would be rate-limiting one. Actually, an oxygen diffusivity in Al_2O_3 and mullite-like layer is much more slower than that in amorphous SiO_2, namely, $\sim 10^{-19}$ in comparison with $\sim 10^{-13}$ cm^2/s for amorphous SiO_2 at 1000 °C (see, e.g.[30]). The peculiarity of oxidation of the Al_2O_3 (ud)-coated Nicalon^{TM} fibers is in the fact that the $(\Delta m)^2/m$–time plot for this process does not obey to the linear dependence after several hours of exposition to air. The deviation may be attributed to the formation of crystalline mullite-like phases in the Al_2O_3–SiO_2 system.[31–33] The oxygen bulk diffusivities in Al_2O_3 and mullite-like phases are the same order values and extremely small,[30] therefore it could be proposed that the diffusion proceed mainly along the grain boundaries. As a consequence, it is strongly dependent on the microstructure of the Al_2O_3-based coatings. The formation of large well-developed crystals and dendrites appear to slow the diffusion (Fig. 7c).

As one can see from Figs. 2 and 3, the ZrO_2 (ud)-coated Nicalon^{TM} fibers are oxidized faster than the Al_2O_3 (ud)-coated fibers. This result is not unexpected because of oxygen diffusivity in ZrO_2 is much faster than that in alumina or mullite and corresponds to 10^{-9} cm^2/ at 1000 °C.[30] No deviation of the $(\Delta m)^2/m$–time plot from linear dependence was observed. It suggests that the mechanism of the oxidation of ZrO_2 (ud)-coated Nicalon^{TM} fibers appears not to be changed as time of exposure to air is increased. Although the interaction of ZrO_2 with SiO_2 at 1000 °C resulting to the formation of $ZrSiO_4$ must not be excluded according to Luecke et al.,[34] the presence of this phase in coating was no demonstrated using XPS and XRD analysis in this study.

The other result to be discussed is the dependence of oxidation resistance of Al_2O_3/ZrO_2-based coatings on sol–gel routes that are used for their formation. Early it was reported by Karakchiev et al.[35] that the properties of sols derived by different ways are distinctive from each other. As was mentioned above, coatings that are obtained using II type sols exhibit more oxidation resistance in comparison with those that are derived from type I (Fig. 4). The reason of this behavior appears to be in the fact that the type II sol exhibits an increased chemical homogeneity, the molecular scale mixing of Al and Zr ions and uniform green microstructure with better control of particle morphology. As a consequence, a more homogeneous composition of coating is produced from this sol. In distinction from the type II, a mixture of separate Al_2O_3 and ZrO_2 sols is no homogeneous one. It could be expected that lower level homogeneity of sols will result in the formation of coatings that are no uniform in composition, microstructure and texture. The appearance of well-faceted crystals on the Al_2O_3/ZrO_2 (type I sol)-coated Nicalon^{TM} fiber is one of an exhibition of non-uniformity.[17] These crystals act as macro defects, break the homogeneity within coating and decrease of the oxidation resistance of coated fiber.

5. Conclusions

A study was conducted to examine the behavior of Nicalon^{TM} fibers with sol–gel derived alumina, zirconia and alumina/zirconia interfacial coatings in air at 1000 °C. Some common and distinctive features of the behavior were detected. In all cases the oxidation is satisfactorily described by the oxygen diffusion-controlled mechanism. Nevertheless, some peculiarities of behavior of oxide interfacial coatings in dependence on type oxides and their prehistory were detected.

The microstructures of oxide coatings derived from sols with low concentration of disperse phase and then exposed to air at 1000 °C are columnar ones, long open pores directed normally to the surface and in some cases, nanosized cracks present. These microstructures provide a diffusion of oxygen inward to the fiber-coating interface along grain boundaries and cracks and this mechanism appears to be predominant at as low temperature as 1000 °C. As a result, an effectiveness of the interfacial coatings derived from sols with low concentration of disperse phase to protection of underlying fiber from further oxidation is not so high. The oxidation rates of Nicalon^{TM} fibers with the interfacial alumina, zirconia and alumina/zirconia coatings exposed to air at 1000 °C are only slightly differed from each other. It was demonstrated that the oxide-based interfacial coatings are distinct in their morphology, defects and adherence to fiber. From this point of view, the ZrO_2 coating appears to be considered as a higher quality one.

The interfacial coatings derived from sols with high concentration of disperse phase retard the oxidation Nicalon^{TM} fibers in a greater extent than those derived from diluted sols. But the presence of defects within coatings can decrease the strength of coated fibers and facilitate an access of oxygen to the fiber-coating interface. Not only concentration of disperse phase but a water as a disperse medium of aqueous oxide-based sols bring influence on the following behavior of oxide-coated Nicalon^{TM} fibers in air at elevated temperatures.

It was found that the oxidation resistance of Nicalon^{TM} fibers with Al_2O_3/ZrO_2-based coatings depends on sol–gel routes that are used for their formation. A higher level of homogeneity of sols results in the formation of coatings that are uniform in composition, microstructure and texture and as a consequence, are more oxidation resistant.

The approach based on using of aqueous-based oxide sols to fabrication of thin coatings on Nicalon fibers^{TM} is inexpensive, accessible and environment-friendly one. It allows us to produce very thin, uniform, adherent and defectless oxide interfacial coatings. This is because of higher level of homogeneity of the initial sols the properties of whose can be readily managed by dilution, number of cycles and other parameters of process. It should be noted that further study is necessary to optimize the process for fabrication of high oxidation resistant coated Nicalon^{TM} fibers.

Acknowledgements

The authors are grateful to T. Gavrilova (Institute of Physics of Semiconductors SB RAS) for SEM analysis, V. Kosheev (Boreskov's Institute of Catalysis SB RAS) for XPS measurements and Dr. A. Sidelnikov for helpful discussion of kinetic data.

References

1. Kerans, R. J., Hay, R. S., Parthasarathy, T. A. and Cinibulk, M. K., Interface design for oxidation-resistant ceramic composites. *J. Am. Ceram. Soc.*, 2002, **85**(11), 2599–2632.
2. Naslain, R. R., The design of the fiber-matrix interfacial zone in ceramic matrix composites. *Composites Part A*, 1998, **29A**, 1145–1155.
3. Singh, R. N. and Brun, M., Effect of boron nitride coating on fiber-matrix interactions. *Ceram. Eng. Sci. Proc.*, 1987, **8**(7/8), 634–643.
4. Naslain, R., Dugne, O., Guette, A., Sevely, J., Robin-Brosse, C., Rocher, J. P. *et al.*, Boron nitride interphase in ceramic matrix composites. *J. Am. Ceram. Soc.*, 1991, **74**(10), 2482–2488.
5. Morscher, G. N., Tensile stress rupture of SiC_f/SiC_m minicomposites with carbon and boron nitride interphases at elevated temperatures in air. *J. Am. Ceram. Soc.*, 1997, **80**(8), 2029–2042.
6. Johnson, D. W., Evans, A. G., Goettler, R. W., Lipowitz, J., Luthra, K. L., Palmer, P. D., *et al.*, *Ceramic Fibers and Coatings: Advanced Materials for the Twenty-first Century*. National Materials Advisory Board, National Academy Press, Washington, DC, 1998.
7. Gundel, D. B., Taylor, P. J. and Wawner, F. E., Fabrication of thin oxide coatings on ceramic fiber by a sol–gel technique. *J. Mater. Sci.*, 1994, **29**(8), 1795–1800.
8. Luthra, K. L., Oxidation-resistant fiber coatings for non-oxide ceramic composites. *J. Am. Ceram. Soc.*, 1997, **80**(12), 3253–3257.
9. Li, H., Lee, J., Libera, M. R., Lee, W. Y., Kebbede, A., Lance, M. J. *et al.*, G.N. morphological evolution and weak interface development within chemical-vapor-deposited zirconia coating deposited on Hi-Nicalon fiber. *J. Am. Ceram. Soc.*, 2002, **85**(6), 1561–1568.
10. Shanmugham, S., Stinton, D. P., Rebillat, F., Bier, A., Besmann, T. M., Lara-Curzio, E. *et al.*, Oxidation-resistant interfacial coatings for continuous- fiber ceramic composites. *Ceram. Eng. Sci. Proc.*, 1995, **16**(4), 389–399.
11. Lee, W. Y., Lara-Curzio, E. and More, K. L., Multilayered oxide interphase concept for ceramic-matrix composites. *J. Am. Ceram. Soc.*, 1998, **81**(3), 717–720.
12. Holmquist, M., Lundberg, R., Sudre, O., Razzell, A. G., Molliex, L., Benoit, J. *et al.*, Alumina/alumina composite with a porous zirconia interphase- Processing, properties and component testing. *J. Eur. Ceram. Soc.*, 2000, **20**(5), 599–606.
13. Li, H., Lee, J. and Lee, W. Y., Effects of air leaks on the phase content, microstructure, and interfacial behavior of CVD zirconia on SiC fiber. *Ceram. Eng. Sci. Proc. B*, 2002, **23**(4), 261–268.
14. Verdenelli, M., Parola, S., Chassagneux, F., Letoffe, J.-M., Vincent, H., Scharff, J.-P. *et al.*, Sol–gel preparation and thermo-mechanical properties of porous xAl_2O_3-$ySiO_2$ coatings on SiC Hi-Nicalon fibres. *J. Eur. Ceram. Soc.*, 2003, **23**(8), 1207–1213.
15. Parola, S., Verdenelli, M., Sigala, K. H. and Scharff, J.-P., Sol–gel coatings on non-oxide planar substrates and fibers: a protection barrier against oxidation and corrosion. *J. Sol.-Gel. Sci. Technol.*, 2003, **26**(1), 803–806.
16. Callender, R. L. and Barron, A. R., Novel route to alumina and aluminate interlayer coatings for SiC, carbon, and Kevlar® fiber-reinforced ceramic matrix composites using carboxylate-alumoxane nanoparticles. *J. Mater. Res.*, 2000, **15**(10), 2228–2237.
17. Baklanova, N. I., Zima, T. M., Naimushina, T. M. and Kosheev, S. V., The formation of refractory oxide coatings on Nicalon^{TM} fiber by sol–gel process. *J. Eur. Ceram. Soc.*, 2004, **24**(10/11), 3139–3148.
18. Kister, G. and Harris, B., *Tensile properties of heat-treated Nicalon and Hi-Nicalon fibres. Composites: Part A.*, 2002.
19. Eaton, H. E. and Linsey, G. D., Accelerated oxidation of SiC CMC's by water vapor and protection via environmental barrier coating approach. *J. Eur. Ceram. Soc.*, 2002, **22**(14/15), 2741–2747.
20. Ophila, E. J., Fox, D. S. and Jacobson, N. S., Mass spectrometric identification of Si-O-OH (g) species from the reaction of silica with water vapor at atmospheric pressure. *J. Am. Ceram. Soc.*, 1997, **80**(4), 1009–1012.
21. Ophila, E. J., Smialek, J. L., Robinson, R. C., Fox, D. S. and Jacobson, N. S., SiC recession caused by SiO_2 scale volatility under combustion conditions: II, thermodynamics and gaseous-diffusion model. *J. Am. Ceram. Soc.*, 1999, **82**(7), 1826–1834.
22. Gu, X., Trusty, P. A., Butler, E. G. and Ponton, C. B., Deposition of zirconia sols on woven fibre performs using a dip-coating technique. *J. Eur. Ceram. Soc.*, 2000, **20**(6), 675–684.
23. *Handbook of X-ray Photoelectron Spectroscopy*, ed. J. F. Moulder, W. F. Stickle and P. E. Sobol. Perkin-Elmer Co., Physical Electronics Division, Eden Prairie, Minnesota, 1992.
24. Powder Diffraction Files (JCPDS—International Centre for Diffraction Data, 1993).
25. Laffon, C., Flank, A. M., Laridjani, P., Hagege, R., Olry, P., Cotteret, J. *et al.*, Study of Nicalon-based ceramic fibers and powders by EXAFS spectrometry, X-ray diffractometry and some additional methods. *J. Mater. Sci.*, 1989, **24**, 1503–1512.
26. Schreck, Ph., Vix-Guterl, C., Ehrburger, P. and Lahaye, J., Reactivity and molecular structure of silicon carbide fibres derived from polycarbosilanes. Part I. Thermal behavior and reactivity. *J. Mater. Sci.*, 1992, **27**, 4237–4242.
27. Schreck, Ph., Vix-Guterl, C., Ehrburger, P. and Lahaye, J., Reactivity and molecular structure of silicon carbide fibres derived from polycarbosilanes. Part II. XPS analysis. *J. Mater. Sci.*, 1992, **27**, 4243–4246.
28. Iler, R. K., *Chemistry of Silica*. John Wiley and Sons, New York, 1979 pp. 62–63.
29. Jarvis, E. A. A. and Carter, E. A., Exploiting covalency to enhance metal-oxide and oxide-oxide adhesion at heterogeneous interfaces. *J. Am. Ceram. Soc.*, 2003, **86**(3), 373–386.

30. Tsai, C. Y., Lin, C. C., Zangvil, A. and Li, A. K., Effect of zirconia on the oxidation behavior of silicon carbide/zirconia/mullite composites. *J. Am. Ceram. Soc.*, 1998, **81**(9), 2413–2420.
31. Schneider, H., Okada, K. and Pask, J. A., *Mullite and Mullite Ceramics*. John Wiley and Sons, England, 1994 pp. 83–90.
32. Tkalcec, E., Ivankovic, H., Nass, R. and Schmidt, H., Crystallization kinetics of mullite formation in diphasic gels containing different alumina components. *J. Eur. Ceram. Soc.*, 2003, **23**(9), 1465–1475.
33. Vioux, A., Nonhydrolytic sol–gel routes to oxides. *Chem. Mater.*, 1997, **9**(11), 2292–2299.
34. Luecke, W., Kohlstedt, D. L. and Dawes, S. B., Oxidation of SiC–ZrO_2 composites. *J. Mater. Sci.*, 1990, **25**(23), 5118–5124.
35. Karakchiev, L. G., Avvakumov, E. G., Vinokurova, O. B., Gusev, A. A., Zima, T. M. and Lyakhov, N. Z., Comparison of sol–gel and mechanochemical techniques to preparation of disperse Al_2TiO_5. *Chem. Sustaining Dev.*, 2001, **9**(1), 27–34.